J Mater Sci: Mater Electron (2010) 21:713–718
DOI 10.1007/s10854-009-9983-3

Synthesis of silver nanorods and application for die attach material in devices

Jinting Jiu · Keiichi Murai · Keunsoo Kim · Katsuaki Suganuma

Received: 29 June 2009 / Accepted: 17 September 2009 / Published online: 26 September 2009

Abstract Silver nanorods have been successfully synthesized in high yield by a polyol process in the presence of $FeCl_3$. The yield and morphology of the silver particles from these conditions were dependant on the concentration of $FeCl_3$, and the molar ratio of the capping agent to $AgNO_3$. The optimized conditions for the synthesis of the nanorods were: 20 μM of $FeCl_3$ and a molar ratio of 1.8:1 of capping agent to $AgNO_3$. The nanorods produced were used to form a silver layer at 400 °C with a low electrical resistivity of 6.1×10^{-6} Ω cm. The silver layer was applied as die-attachment films to connect a SiC chip to a copper substrate. This formed a porous structure, which was evaluated for structure and strength.

1 Introduction

The design and selection of die-attach material has become critical to ensure device robustness and reliability in the modern electronics industry due to the need to improve cost-efficiency, fastness and miniaturization. Die-attach materials can also be used to do more than simply attach the die to the die pad, substrate, or cavity. They can also provide a good thermal and/or electrical connection between the die and the package, affecting the performance of the devices while operating in commercial and domestic electric appliances. Thus, materials with better electrical, thermal and thermomechanical properties for semiconductor products need to be developed. Among those new materials, silver-based attachment pastes are excellent candidates due to their high thermal and electrical conductibility [1–4]. However, the high sintering temperature (>500 °C) of the current commercial silver pastes makes them unsuitable for interconnections in semiconductor devices. On the other hand, nanoscale materials are known to sinter at lower temperatures due to their larger surface areas [5, 6]. Therefore, a nanoscale silver paste has the potential to be a lead-free, low temperature sintering, high-performance die-attach material that would be especially suitable for bonding semiconductor devices to metalized substrates. In the present work, a novel die-attach material is presented, made from silver nanorods that were synthesized with a polyol process method.

One-dimensional (1-D) metal nanostructures, such as nanorods, nanowires and nanotubes, are also of interest because of their unique electronic, optical, magnetic, thermal, and catalytic properties [7, 8]. Much effort has been made recently to control their structure as the desirable properties, which are distinctive from the bulk solids, are related to their small sizes and well-defined shapes [9, 10]. As for silver nanostructures, a variety of shape-controlled syntheses have been developed. These are capable of producing silver nanoplates, nanoprisms, nanorods, and nanowires. Recently, a polyol process has attracted more attention due to its simplicity and ease of operation in an air environment [11–13]. However, reports have suggested that some seeds and salts affected the morphology of the products [14–16], although the mechanism is still unclear. The focus of the present study is on how the salts affect the preparation of 1-D silver nanorods and on the elucidation of the growth process for the nanorods in the polyol process. Finally, these silver nanomaterials were used to form a silver paste and were used in a die-attaching technique for semiconductor devices.

J. Jiu (✉) · K. Murai · K. Kim · K. Suganuma
Institute of Scientific and Industrial Research, Osaka University, Ibaraki, Osaka 567-0047, Japan
e-mail: jiu@eco.sanken.osaka-u.ac.jp; jiujinting@hotmail.com

2 Experimental process

In a standard synthesis [14], 6 mL of ethylene glycol, acting as both reducing agent and solvent, with 0.052 M $AgNO_3$ and 0.067 M polyvinylpyrrolidone (PVP, average molecular weight: 360 k) was mixed with 0.5 mL of $FeCl_3$ solution (6×10^{-4} M, in ethylene glycol) at room temperature and then heated at 150 °C on an oil bath for 1.5 h. Finally, to completely remove the capping agent (PVP) and organic compounds formed in the reaction, the resulting was diluted with large volume of acetone and ethanol and the silver particles collected by centrifugation at 2,000 rpm for 10 min. This washing process was repeated to ensure purity. The silver precipitates in ethanol were characterized by scanning electron microscopy (SEM; JEOL, JSM-5510S). Electronic absorption spectra were taken at room temperature with a Jasco V-570 spectrometer using a 1-cm optical path quartz cuvette by diluting 0.3 mL of the sample solution to 1 mL. The X-ray powder diffraction (XRD) patterns were recorded using a Rigaku RINT 2500 diffractmeter with Cu Kα radiation over a 2θ range from 20° to 80°. For XRD, precipitation samples in ethanol were dropped onto a glass substrate to form a thin film. Similarly, a drop of the ethanol sample was put on a grid covered with a carbon film for transmission electron microscopy (TEM; JEOL 200CX).

3 Results and discussion

3.1 Properties of the prepared Ag nanoparticles

Figure 1 shows the SEM images of the silver particles obtained from the synthesis using $FeCl_3$ (Fig. 1a) and without it (Fig. 1b). With $FeCl_3$, the silver nanorods were several micrometers in length and about 75 nm in diameter. However, without $FeCl_3$, the silver particles were a mixture of small particles, from 100 to 300 nm in size, and larger, elongated particles. Figure 1c presents the XRD pattern of both types of silver particles. All the peaks can be indexed to the FCC structure of single crystal bulk silver (International Center for Diffraction Data, PDF # CA-0783). The lattice constant calculated from the XRD data ($a = 4.090$ Å) is very close to the reported value ($a = 4.0862$ Å). It is worth noting that the ratio of the intensity of the (111) and (200) peaks is higher for the nanorods than that of the nanoparticles, indicating the (111) planes are enriched in the Ag nanorods. This shows the morphology of Ag particles can be controlled by the addition of $FeCl_3$.

The morphology and yield of the silver nanoparticles are affected by the molar ratio of capping agent (PVP) to $AgNO_3$ as well as the concentration of $FeCl_3$ [14]. With a molar ratio of PVP/$AgNO_3$ in the range of 0.7–1.8, nanorods were the dominant product with a length and diameter similar to that shown in Fig. 1a. High concentrations of PVP may form a tight cover on all the faces of the growing silver particles, leading to isotropic growth. Conversely, low concentrations of PVP results in a decrease in coverage and gives anisotropic growth of wide and short rods.

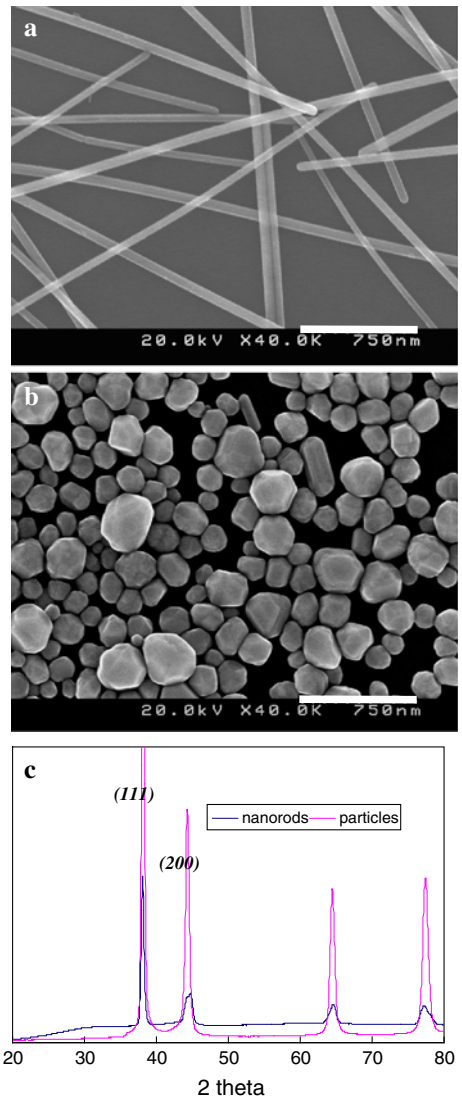

Fig. 1 SEM images and XRD pattern of silver particles: **a** with $FeCl_3$, **b** without $FeCl_3$ and **c** their XRD

Figure 2 shows SEM images of two extreme products from changes in the concentration of $FeCl_3$. The standard procedure was used with a PVP/$AgNO_3$ molar ratio of 1.28 and the $FeCl_3$ concentrations of 10 and 52 μM, in Fig 2a and b, respectively. At low concentrations of $FeCl_3$, the product is a mixture of spherical and rod-shaped particles. The yield of 1-D nanorods was almost 50% (Fig. 2a). When the concentration of $FeCl_3$ was increased to 52 μM, very short and wide rods including some large irregular

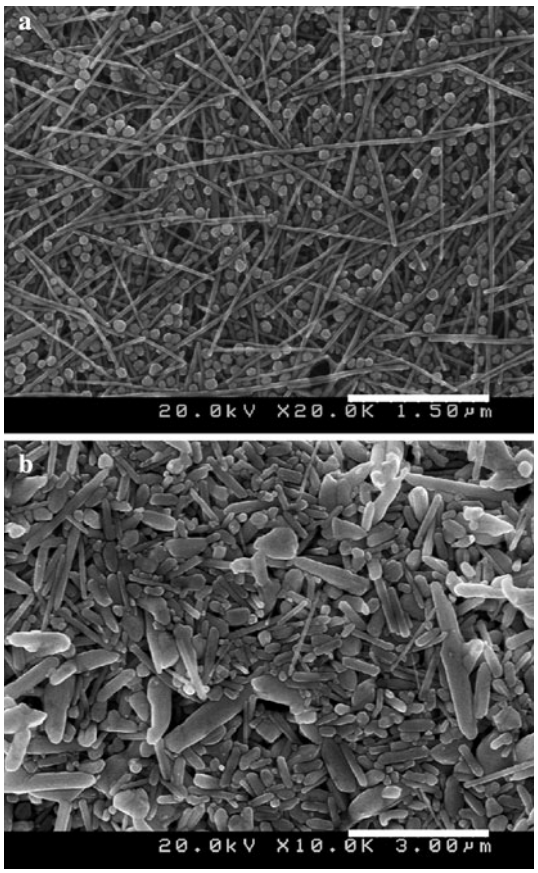

Fig. 2 SEM images of silver nanoparticles prepared with the concentration of $FeCl_3$ at 10 μM (**a**) and 52 μM (**b**)

particles were the main products (Fig. 2b). Below 10 μM of $FeCl_3$, nanorods were not obtained. Long silver nanorods were consistently obtained when the concentration of $FeCl_3$ was in the range of 18–24 μM. From these results, one can see that the $FeCl_3$ salt affects the morphology of the silver nanoparticles from the polyol process. Xia et al. have reported the even a very small amount of $Fe^{2+/3+}$ ions drastically affects the yield and shape of silver nanowires by removing oxygen from the surface of silver seeds and preventing the dissolution of silver nucleoli [16]. To determine if $Fe^{2+/3+}$ ions are crucial in the synthesis of nanorods, or if other metals could achieve similar results, the experiment was repeated with NaCl, $ZnCl_2$, $NiCl_2$, $CoCl_2$ and $CuCl_2$ salts as the additives. Similar results were obtained as in the case of $FeCl_3$, with a similar dependency on the concentration. However, not all these metal ions have different valences available, as Fe^{2+} and Fe^{3+} ions do [16], indicating an oxidation process could not be responsible for the selectivity for nanorods. Other salts, such as $NiNO_3$, $ZnNO_3$, $NaNO_3$ and Na_2SO_4 salts were also tested for the formation of nanorods. Although some five-twinned crystals were observed in the beginning of the synthesis, long nanorods were not formed. Short rods were observed in the final product about 300 nm in length and 120 nm in diameter, which is similar to those obtained in the absence of $FeCl_3$. These results suggest that the main reason for the formation of silver nanorods is the chloride anions and not the Fe^{2+} or Fe^{3+} ions.

To test that it is the anion which is controlling the process, CO_3^{2-} and S^{2-} ions, from Na_2CO_3 and Na_2S were also tested. Nanorods, similar to those from $FeCl_3$, were the main product and again, the product was dependant on the concentration of the anion. All these salts, including the earlier chlorides, form an Ag_xA_y (A is anion ions) precipitate at the start of the reaction. Thus, it seems that the formation of silver nanorods is related to the dissolution of this precipitate. However, the relationship between Ag_xA_y and the morphology of resulted Ag particles is still unclear. Experiments into this result are ongoing.

3.2 Properties of Ag paste

These silver products were applied as a paste for the fabrication of a silver layer to demonstrate the sintering properties and structure of silver layers in an electronic device. Firstly, these silver precipitates were washed with acetone and ethanol to completely remove PVP and other impurities. Figure 3 shows the thermal analysis data of the silver nanorods precipitate before and after the wash process. The DTA results for the rods before the wash show an exothermic peak at about 400–450 °C. This corresponds to the decomposition of PVP with a dramatic weight loss in the TG curve. A strong endothermic peak was also seen at about 490 °C, which is typical for nano-sized products. After the wash, almost no PVP exothermic peak can be observed, which suggests the PVP has been completely removed. However, a new endothermic peak appears at about 300 °C with a very small weigh loss of about 2.1%, which may correspond to the removal of the PVP directly on the surface of the nanorods. The reason the surface PVP decomposition occurs at a much lower temperature than bulk PVP is still unclear.

A silver paste was formed by addition of a small amount of ethanol to the precipitate obtained by centrifugation. To prepare a silver layer, the silver paste was spread onto a glass substrate, dried at room temperature for several minutes and sintering at the desired temperature for 60 min in an oven. After treatment, the electrical resistivity (ER) of the silver thin film was examined with four point probe resistance measurements. Table 1 shows the results for the pure nanorods (PN) and a mixture of nanorods (about 50%) and spherical particles (MN). The resistivity is decreased with increasing sintering temperature in the two pastes. However, the pastes exhibit high resistivity at low temperature despite the layer being pure metal silver. This may be due to poor sintering between particles. The SEM image

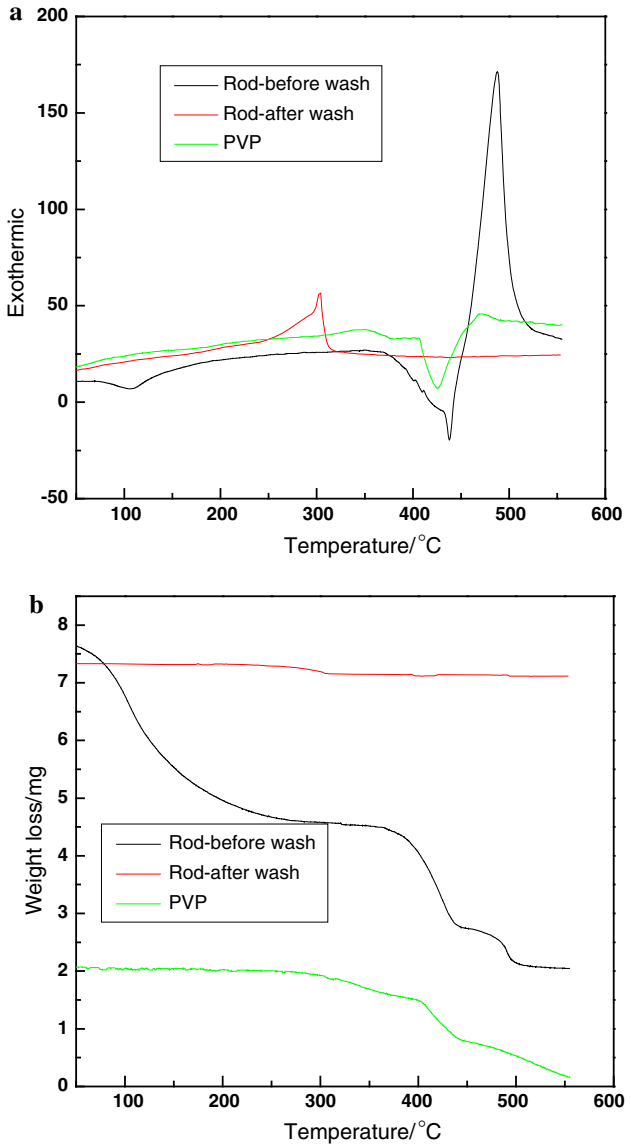

Fig. 3 The DTA (**a**) and TG (**b**) results of Ag nanorods for sample before washing and after washing in comparison with PVP

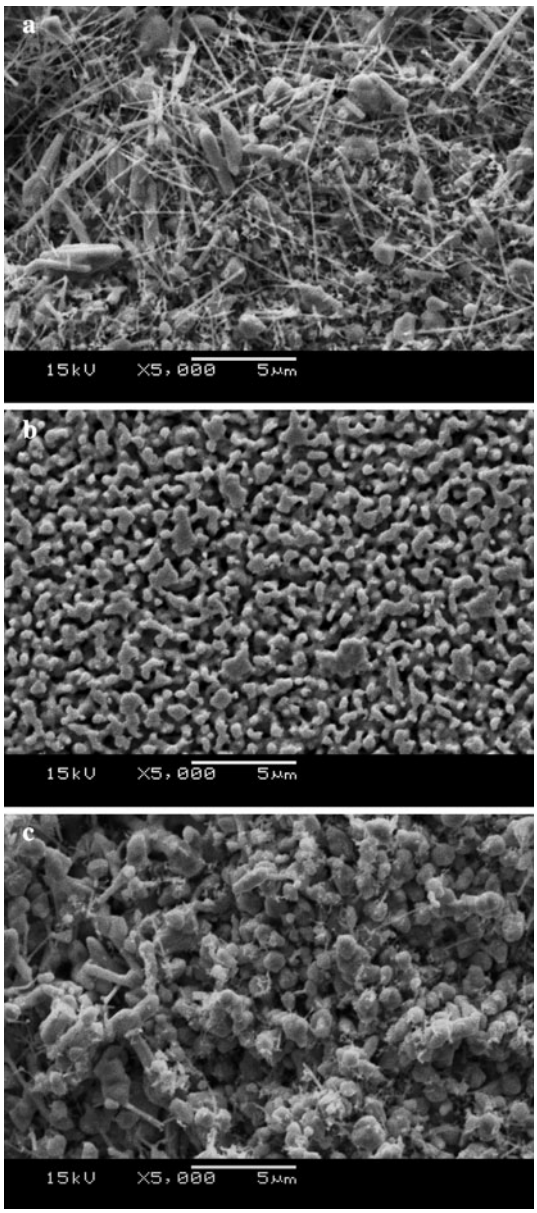

Fig. 4 The SEM images of Ag layers with PN (**a**) and MN (**b**) sintered for 1 h at and 300 °C, and PN (**c**) sintered for 10 h at 300 °C

Table 1 Resistivity of nanorods and nanoparticles layer

Resistivity (Ω cm)	PN	MN
200 °C	5.3×10^{-3}	3.6×10^{-3}
300 °C	1.7×10^{-4}	6.5×10^{-5}
400 °C	6.1×10^{-6}	3.2×10^{-6}

of the silver thin film indicated that the rod morphology was retained from the PN paste (Fig. 4a) but destroyed in the MN paste (Fig. 4b) after sintering at 300 °C for only 1 h. The later consisted of a dense network microstructure. However, when the sintering time was extended to 10 h, the rod-shape particles in the PN paste form irregular 0-dimension particles with different sizes, including some rod-shape particles (Fig. 4c). Comparing Fig. 4b and c, it can be seen that the grain growth and increase in density is lower in the PN paste than in the MN paste. The results suggested that pure nanorods are more difficult to sinter and that this gives a higher resistivity at the same sintering temperature due to the poor connection between the particles. The sintering properties of PN and MN paste will be discussed in depth in later reports.

The silver layer prepared form the PN paste has been trialled as a die-attach material. It was coated onto a copper substrate to connect it to a SiC chip by sintering at different

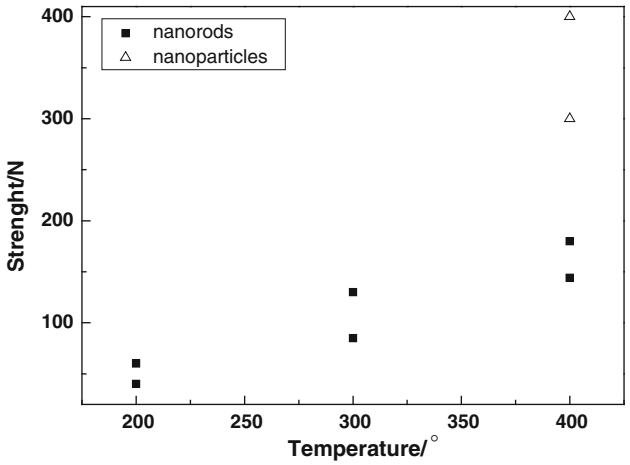

Fig. 5 The joint strength of nanorods and nanoparticles layers as fuctions of sintering temperature

temperatures for 1 h and examined for joint strength. Figure 5 showed the results. Although the strength is increased with the temperature, the strength of silver nanorod layer is very low compared with the nanoparticle sample. The surface and cross-section structure of the Ag nanorod and nanoparticle samples which had been calcined at 350 °C (nanoparticles were provided by Harima Chemicals INC, Japan) were observed by SEM (Fig. 6). The surface state was completely different in the two cases. The nanorods sample formed a porous structure by the nanorods breaking and fusing into a network structure at contacts between rods (Fig. 6a). The nanoparticles achieved a denser packing structure due to sintering between particles (Fig. 6b). On the other hand, the cross-section SEM images also indicated that a mesoporous structure has been formed from the nanorods and a dense packing structure from the nanoparticles (Fig. 6c, d). At the highest magnification (in Fig. 6c), it can be seen the pores have been formed by the breaking and connecting of the nanorods with the heating process. The pore size ranged from 0.2 to 2 μm depending the sintering process and temperature. These pores are the main reason for the low strength. Normally, porous materials have lower strengths than those of denser materials. However, the two cases show almost same resistivity at high temperature, which is similar to that of bulk silver materials. The results indicate the porous silver structure has same capacity to transport electrons. Compared to the dense packing structure of nanoparticles, the mesoporous structure appears to be the most promising route for high performance attachment materials because of the rapid transport and diffusion of heat and electrons through the layer. However, the low strength of the Ag layer will affect the lifetime of the device. Hence, improving the utilizing strength will be a challenge for the application of these porous die-attach materials in semiconductor devices.

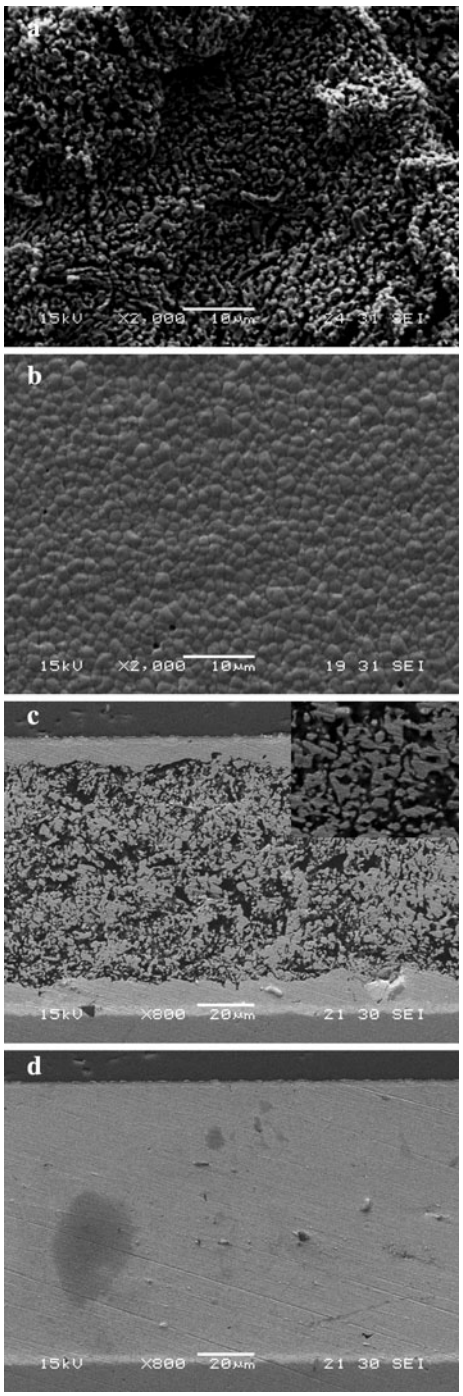

Fig. 6 The surface and cross-section SEM images of nanorods (**a**, **c**) and nanoparticle (**b**, **d**), respectively

4 Conclusion

The Ag nanorods with high yield have been successfully synthesized by addition of inorganic salts with the polyol process. We discussed the growth mechanism that these anion ions improved the formation of Ag nucleus into rod-shape particles in the beginning state by dissolving and

assembling the Ag nucleus. These results also implied that the other metal with different morphology will be prepared if suitable inorganic salts, i.e., anions, have been selected.

The Ag products including different percent of Ag nanorods were used to form an Ag layer at 400 °C to connect a chip to substrate. The electrical resistivity depended the sintering temperature and a low resistivity of about 6.1×10^{-6} Ω cm has been achieved for pure nanorods samples, which is little higher than that one of 3.2×10^{-6} Ω cm including about 50% nanorods sample. The layer is a porous structure that will provide the quickly transport and diffusion of heat and carriers in the electronic devices. However, the low strength of the layer will be next study challenge for improving the utilizing in semiconductor devices.

Acknowledgments The authors are gratefully acknowledged Professor S. Isoda and M. Adachi for helpful discussions. We would like to thank Dr. Ohashi and Dr. Arai for their help in preparing the work. This work was performed as a part of Development of Inverter Systems for Power Electronics project supported by the NEDO (New Energy and Industrial Technology Development Organization, Japan).

References

1. S. Rane, V. Puri, D. Amalnerkar, J. Mater. Sci. Mater. Electron. **11**, 667 (2000)
2. C.R. Chang, J.H. Jean, J. Amer. Ceramic Soc. **81**, 2805 (1998)
3. Z. Zhang, G. Lu, IEEE Trans. Electron. Packag. Manuf. **25**, 279 (2002)
4. R.W. Chuang, C.C. Lee, IEEE Trans. Compon. Packag. Technol. **25**, 453 (2002)
5. J.G. Bai, Z. Zhang, J.N. Calata, G. Lu, IEEE Trans. Compon. Packag. Technol. **29**, 589 (2006)
6. J.R. Groza, A. Zavaliangos, Rev. Adv. Mater. Sci. **5**, 24 (2003)
7. J. Chen, B. Wiley, Y. Xia, Langmuri **23**, 4120 (2007)
8. A.M. Morales, C.M. Lieber, Science **279**, 208 (1998)
9. M. Bockrath, W. Liang, D. Bozovic, J.H. Hafner, C.M. Lieber, M. Tinkham, H. Park, Science **291**, 283 (2001)
10. R. Jin, Y. Cao, E. Hao, G.S. Metraux, G.C. Schatz, C.A. Martin, Nature **425**, 487 (2003)
11. C. Fischer, A. Heller, G. Dube, Mat. Res. Bull. **24**, 271 (1989)
12. C. Ducamp-sanguesa, R. Herrera-urbina, M. Figlarz, J. Solid State Chem. **100**, 272 (1992)
13. Y. Sun, Y. Xia, Science **298**, 2176 (2002)
14. J. Jiu, K. Murai, D. Kim, K. Kim, K. Suganuma, Mater. Chem. Phys. **114**, 333 (2009)
15. B. Wiley, T. Herricks, Y. Sun, Y. Xia, Nano Lett. **4**, 1733 (2004)
16. B. Wiley, Y. Sun, Y. Xia, Langmuir **21**, 8077 (2005)